Enhancing Motor Imagery Performance by Antiphasic 10 Hz Transcranial Alternating Current Stimulation

Lei Zhang, Long Chen, Zhongpeng Wang, Xiuyun Liu, and Dong Ming, *Senior Member, IEEE*

Abstract—**Motor imagery (MI), as a cognitive motor process, involves the coordinated activation of frontal and parietal cortices and has been widely studied as an effective way to improve motor functions. However, there are large inter-individual differences in MI performance, with many subjects unable to elicit sufficiently reliable MI brain patterns. It has been shown that dual-site transcranial alternating current stimulation (tACS) applied on two brain sites can modulate functional connectivity between the targeted regions. Here, we investigated whether electrically stimulating frontal and parietal regions using dual-site tACS at mu frequency will modulate motor imagery performance. Thirty-six healthy participants were recruited and randomly divided into in-phase (0° lag), anti-phase (180° lag) and sham stimulation group. All groups performed the simple (grasping movement) and complex (writing movement) motor imagery tasks before and after tACS. Simultaneously collected EEG data showed that the event-related desynchronization (ERD) of mu rhythm and classification accuracy during complex task were significantly improved after anti-phase stimulation. In addition, anti-phase stimulation resulted in decreased event-related functional connectivity between regions within frontoparietal network in the complex task. In contrast, no beneficial after-effects of anti-phase stimulation were found in the simple task. These findings suggest that dual-site tACS effects on MI dependent on the phase lag of the stimulation and the complexity of the task. Anti-phase stimulation applied to the frontoparietal regions is a promising way to foster demanding MI task.**

Index Terms—**Motor imagery, EEG, transcranial alternating current stimulation, functional connectivity.**

I. INTRODUCTION

MOTOR imagery (MI) refers to the internal simulation of a given action without the actual corresponding motor output, and it has been widely used as a mental training tool in the fields of sport and motor rehabilitation [1], [2], [3]. In particular, motor imagery based brain-computer interface (MI-BCI) can correlate the motor intentions with afferent signals from external devices to active neuroplasticity, thereby improving motor performance and facilitating neurorehabilitation [4], [5]. As a mental rehearsal of limb movement, motor imagery (MI) can induce an extensive activation of motor related cortex [6], [7]. The cortical activities generated by MI are usually characterized as a power suppression (event related desynchronization (ERD)) or a power enhancement (event related synchronization (ERS)) of mu and beta rhythm. Although, the ERD patterns should appear consistently during MI, this is not always the case. There are large inter-individual differences in MI performance, not all individuals can elicit sufficiently pronounced ERD, which impedes the widespread application of MI-BCI [8]. Therefore, it is important to develop appropriate strategies to improve MI performance, and thus facilitate the practical applications of MI-BCI.

In the past decades, intensive studies have been devoted to improving MI-BCI accuracy. For instance, signal processing algorithms have been greatly improved to enhance the ability to identify MI patterns [9], [10]. Despite some advances in these algorithms, the application of MI-BCI is still limited by the inability of some subjects to generate reliable neural response patterns. Therefore, some researchers have concentrated on developing appropriate MI guidance approaches to assist users in performing MI correctly. Approaches such as neuromuscular electrical stimulation acting on peripheral limbs, as well as vibrational stimulation, have been shown to provide somatosensory afference and modulate cortical activity [11], [12]. In addition, as a non-invasive neuromodulation technique, transcranial electrical stimulation (tES) has also attracted attention of researchers recently. Transcranial direct current stimulation (tDCS) can regulate cortical excitability by applying low-level currents to the brain through scalp electrodes. Depending on the stimulation polarity acting on a specific cortex, tDCS can induce different effects on cortical excitability [13]. Several

studies indicated that tDCS can induce significant changes in power of mu and beta rhythm during MI [14], [15]. In contrast, transcranial alternating current stimulation (tACS) applies a weak sinusoidal electrical current to the cerebral cortex and regulates cortical excitability in a frequency-specific manner. Wach et al. showed that 10 Hz tACS applied to the primary motor cortex could enhance motor performance and improve motor cortical excitability [16]. Feurra et al. indicated that corticospinal excitability during MI could be facilitated by theta and alpha tACS [17]. These findings suggest that non-invasive neuromodulation technique acting on cerebral cortex is an effective way to modulate cortical rhythmic activity.

Although previous studies have shown that changes in cortical excitability can be induced by applying tES to the motor-related cortex, it has been neglected that modulation of intercortical interactions may also affect cortical excitability. Neuroimaging studies in humans have revealed that inter-regional interactions are essential to most brain functions and associated with working memory, attentional state and task demands [18], [19], [20], [21]. In particular, the frontoparietal network (FPN), consisting of the lateral prefrontal cortex and posterior parietal cortex, is assumed to be involved in a wide variety of high-level cognitive processes [22]. As a cognitive motor process, MI also involves functional connectivity (FC) changes in the frontoparietal network. Zhang et al. demonstrated that functional connectivity patterns in the frontoparietal attention network are related to individual MI-BCI performance [23]. Recently, Ogawa et al. used the causal discovery approach to estimate the functional connectivity networks underlying motor execution (ME) and MI [24]. Their results indicated that the parietal regions can receive movement-related information from prefrontal regions, implying large-scale interactions across bilateral frontoparietal networks during ME and MI. By applying Granger causality mapping, several studies have also identified functional relationships in the frontoparietal network during MI [25], [26].

Communication between distant brain regions is widely believed to take place through oscillatory activity, which appears to simultaneously orchestrated activity across distant regions during cognitive processes [27]. Oscillatory synchrony within and between frequency bands is regarded as the foundation for large scale network integration [28], [29]. Specifically, long-range frontoparietal interactions during mental imagery evolved in the theta and alpha frequency range, whereas local and short-range integration seem to involve gamma frequency dynamics [30]. Recently, dual-site tACS has been used to modulate oscillatory synchrony between brain regions by selectively injecting weak alternating currents into two brain regions. The two primary stimulation conditions are in-phase synchrony (0° phase shift between the two regions) and anti-phase synchrony (180° phase shift between the two regions). In-phase stimulation serves to integrate separated functions in different regions by synchronizing the endogenous oscillations [19], [31]. On the contrary, anti-phase stimulation is thought to desynchronize the neural oscillations between the two brain regions, causing some brain regions to increase activity while others to reduce activity [18]. Several

studies have demonstrated that dual-site tACS applying on the frontoparietal network can affect the performance of a variety of tasks such as working memory [19], [31], visual attention [32] and value-base choices [33]. However, it remains unclear whether MI-BCI performance can also be regulated by dual-site tACS intervention acting on frontoparietal network.

In the present article, we set out to determine whether MI performance can be improved after artificially manipulating the oscillatory synchrony between the frontal and parietal cortices. Dual-site tACS at mu frequency (10 Hz) was used to entrain endogenous oscillations and modulate intercortical interactions. The effects of in-phase and anti-phase stimulation were assessed in this study and a sham stimulation condition was set to control placebo-like effects. We clarified the effect of dual-site tACS mainly by comparing the ERD and BCI accuracy during MI before and after stimulation. The aftereffects of alpha-tACS have been reported to last for at least 30 minutes [34]. In addition, interactions between cortical areas may vary depending on the complexity of the motor task [35]. We developed simple and complex MI tasks in this study to test whether the tACS effect varies with task complexity. Taken together, we hypothesize that dual-site tACS with different phase shift have varied effect on MI performance, and the effect of tACS may be affected by task complexity.

II. METHODS

A. Participants

Thirty-six right-handed healthy subjects (14 females, age 24.6±2.1) with normal or corrected to normal vision took voluntary part in the experiment. The study was approved by the ethical committee of Tianjin University. Subjects gave their written consent and were fully informed about the experiment procedure prior to the participation. Participants did not report any neurological disorder according to their statements. Only participants being naive to transcranial electrical stimulation methods were chosen.

B. Electroencephalography Recording

The EEG data were recording using a SynAmps 2 system (Neuroscan, Victoria, Australia) with 60 standard Ag/AgCl electrodes. The electrodes were arranged according to the 10-10 standard configuration. The reference electrode was placed on nose and the ground electrode was positioned on the forehead. EEG signals were sampled at 1000 Hz with a notch filter to filter out the interference of power supply at 50 Hz. The impedance was modulated to less than 10 kΩ during the EEG data acquisition process.

C. tACS Protocol

Transcranial alternation current stimulation was applied via two ring-shaped conductive rubber electrodes covered with saline soaked sponges from stimulator system (DC-stimulator Plus, Neuroconn, Ilmenau, Germany). The outer diameter of the rubber electrodes is 48 mm and the inner diameter is 24 mm (area: 15 cm2). The stimulation electrodes were placed over the right prefrontal (F4) and parietal (P4)
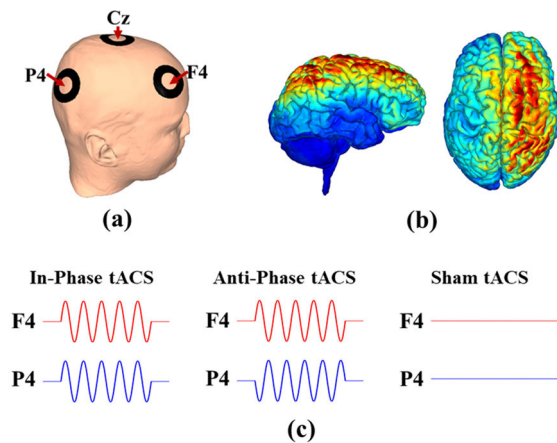
Fig. 1. Experimental stimulation setups. (a) Dual-site tACS montage. Electrodes were placed at frontoparietal sites F4 and P4 with a common return at Cz. (b) Three-dimensional representation of dual-site tACS electric field on the cortical surface. (c) Stimulation conditions. Dual-site tACS was applied at 10 Hz frequency with 0° relative phase between F4 and P4 in the in-phase condition and with 180° relative phase in the anti-phase condition. Stimulation was applied for 20 min except for the sham condition where current was only applied for 30s.

cortices, with the return electrode at Cz (Fig. 1(a)). The multi-channel stimulator system used in this study ensured that each stimulation electrode connected to one independent channel. The EEG cap was affixed on top of the stimulation electrodes such that the EEG recording electrodes were exactly located in the centre of the ring-shaped stimulation electrodes. A sinusoidal waveform with intensity of 1 mA (peak-to-peak) was applied for a total duration of 20 min. The stimulation frequency was set to 10 Hz (within the mu range). The SimNIBS software package was used to simulate the electric field distribution during tACS (Fig. 1(b)) [36].

The three stimulation conditions were illustrated in Fig. 1(c). In-phase condition applied dual-site tACS over prefrontal and parietal regions with a relative phase difference of 0°. Anti-phase condition applied dual-site tACS with a relative phase shifted by 180°. Sham condition had the same current amplitude and phase difference as in-phase condition, with the difference that current was only applied for 30s. For all three conditions, the current was ramped up and down in the initial and last 30s of stimulation, respectively. After the stimulation, the questionnaire by Violante et al. was used to assess possible adverse effects of tACS [19].

D. Experimental Tasks and Procedures

Thirty-six participants were randomly divided into three groups in a parallel group design (twelve participants in each group), with each group receiving either in-phase, anti-phase or sham stimulation. The experimental procedures were similar in all groups. As illustrated in Fig. 2 (a), the experiment consisted of three blocks. Before the stimulation (pre-tACS block), participants' EEG was recorded during the simple and complex motor imagery tasks. Then, stimulation was turned on for 20 min and participants were instructed to remain at rest during the stimulation. At the end of the stimulation (post-tACS block), EEG was recorded during the same experimental tasks as pre-tACS block.

In this study, two MI-related tasks were developed according to Mashat et al.'s study: simple task (ST) and complex task (CT) [37]. The simple task was characterized as a grasping movement that participants were instructed to perform kinaesthetic imagery of left-hand grasping movement without causing muscular contraction. Since grasping movement is more regularly employed in the daily life of healthy people, it may involve less cognitive activity in the brain [37]. The complex task was characterized as a writing movement. Participants were asked to kinaesthetically imagine writing an English letter which appeared on the screen using their left hand and avoid limb activities. The CT contained four different English letters: "A", "E", "Q" and "S". In principle, a complex task requires a higher cognitive load than a simple task, which may impact the intensity and location of brain activation. The main reason for adopting the non-handed tasks is to expand the complexity of performing the two MI tasks. In addition, the experiment included a rest task which was characterized as the participants being completely relaxed without any intention of moving.

The timing of a MI task trial is presented in Fig. 2(b) and Fig. 2(c). At the beginning of each trial, a green cross appeared in the centre of the screen as a preparation signal for the task and lasted for 1 second. At this stage, the participants were instructed to relax and prepare for the task. Then, a cue in the form of a green cross with blue arrow was presented on the screen indicating the type of MI task. If the term "grasping" appeared under the cross, it suggested that MI task was ST, whereas the term "writing" indicated that the MI task was CT. This cue lasted for 1 s, followed by a green cross with a red arrow was shown on screen for 4 s. During this period, participants were required to imagine the grasping movement of the left-hand if the task was ST. For the CT, participants were asked to perform kinaesthetic imagery of writing the letter that appeared on the arrow in this time. The task was finished once the screen went black. The trial flow of the rest task is shown in Fig. 2(d). Similar to the MI task, the trial began with a green cross appearing on the screen for 1s. After then, the green cross lingered on the screen for 4s before disappearing. In this period, participants were induced to stay at rest. The screen then turned black to indicated the end of the trial. The inter-trial intervals were set at random between 3 and 5 s to prevent adaptation, during which only a black screen was presented. Participants completed 5 runs in each of pre-tACS and post-tACS blocks. Each run included twenty-four trials (8 trials ST, 8 trials CT and 8 trials rest task), which were performed in a random order. There was a total of 40 trials per task at the end of each block. Across 40 trials in total for CT, each English letter appeared 10 times. During the experiment, participants were instructed to sit in a relaxed and comfortable position with their hands naturally resting on the armrests. A 24 inch monitor was placed 80 cm in front of the participants to provide visual instructions. During task period, participants were informed to restrict their movements, such as blinking or swallowing, which may produce artifacts.
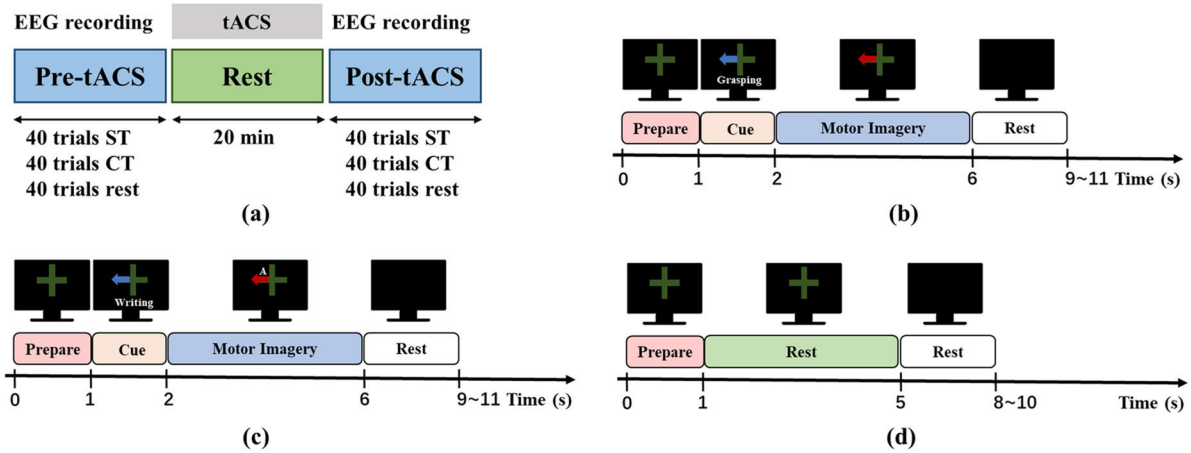
Fig. 2. Experimental design. (a) The time course of experimental phases. (b) Single-trial procedure of the simple task (ST). Subjects were required to perform motor imagery of left hand grasping movement according to the cue. (c) Single-trial procedure of the complex task (CT). Subjects were asked to perform motor imagery of left hand writing movement. (d) Single-trial procedure of the rest task. Subjects were required to remain completely relax.

E. EEG Preprocessing

Preprocessing of the EEG data was carried out by the EEGLAB toolbox [38]. For decoding analysis, raw EEG data were only band-pass filtered into 8 to 12 Hz and down sampled to 250 Hz. For the rest of the analysis, raw EEG data were first low-pass filtered below 200 Hz. Due to the high-pass filtering may cause dependencies among surrounding data samples, it is not applied in preprocessing. Instead, the data trends were eliminated using piecewise-linearly detrending with a 330 ms window every 82.5 ms. The data were then down sampled to 500 Hz. Next, bad channels (detected by visual inspection) were interpolated by the spherical spline interpolation method implemented in the EEGLAB. After that, independent component analysis (ICA) was performed to remove artifacts caused by eye movements and muscle activity. The rank-deficiency problem was addressed by reducing the number of ICs. Spherical spline laplacian, also known as current source density (CSD), was then used to eliminate the low-frequency coupling among EEG recording electrodes. This was accomplished using the Perrin et al.'s method [39], as implemented in the CSD toolbox [40]. Following that, data segments contaminated by artifacts were identified by visual inspection and manually removed by using EEGLAB.

F. Feature Extraction and Classification

BCI performance was evaluated by the decoding accuracy between the MI-related and rest states. The MI-related state was extracted from 2s to 6s of each MI task trial and rest state was extracted from 1s to 5s of each rest task trial. The common spatial pattern (CSP) algorithm was then utilized to extract EEG features from all 60 electrodes. The CSP is a supervised method to extract discriminative spatial feature from EEG by maximizing the variance of one class and minimize the variance of another class. The first and last four log variance features generated by CSP algorithm were chosen as feature vectors. After the CSP procedure, a linear support vector machine (SVM) classifier with the regularization parameter C of 1 was trained to distinguish between MI-related state and

rest state. One classifier was trained to discriminate ST from rest task, and another classifier was used to discriminate CT from rest task. During the decoding analysis, a 10 × 10-fold cross-validation method was applied to evaluated the classifier performance of each block. The 80 trials of two class were randomly divided into forty sets, with each set including a MI-related task sample and a rest task sample. At each round of 10-fold cross validation, forty sets were randomly divided into ten equally sized segments. At each fold, nine segments were used to train the classifier and the resting one segment was used for testing. This produced 10 different classification accuracies, which were then averaged. In order to minimize the potentially severe overfitting, CSP filters were computed repeatedly on the training set within each fold. The same round was repeated ten times and each subject's final classification performance was evaluated using the average of all round classification accuracies.

G. Time-Frequency Analysis

In order to evaluate the effect of tACS on cerebral cortex activity, we compared the event-related spectral perturbation (ERSP) of EEG data between pre-tACS and post-tACS blocks for three stimulation groups. ERSP has been widely utilized to represent spectrum power changes of EEG signals in the time-frequency domain [41]. In a defined frequency band, the increase or decrease in power relative to baseline can be represented in the form of ERS or ERD. The ERSP was generally formulated as follow:

$$ERSP(f, t) = \frac{1}{n} \sum_{k=1}^{n} F_k(f, t)^2 \qquad (1)$$

where n is the number of trials, and $F_k(f, t)$ is the spectral estimation of kth trial at frequency f and time t. The short-time Fourier transform (STFT) with a Hanning-tapered window from EEGLAB was used to compute the ERSP. ERSP values were then log-transformed and normalized by subtracting the mean power during baseline period. The baseline period was set between 0.2 and 1 second before the appearance of preparation signal (from -1 to -0.2 s).

The ERSP analysis were carried out by extracting the power spectrum changes for frequency bands 3-35 Hz and time period from -2 to 7 s. Then, the averaged ERSP values over trials per task in each EEG recoding electrode was computed. The ERSP values at contralateral key electrode C4 were mainly analyzed. Furthermore, in order to quantify the ERD patterns, we calculated the ERD values in electrode C4 by subtracting power spectrum at baseline from power spectrum during task period (2-6 s) and dividing by the same baseline power spectrum. The ERD values were then averaged across task period and across mu (8-12 Hz) and beta (14-30 Hz) frequency bands. A mixed design 2×3 ANOVA with block (pre-tACS block, post-tACS block) as a within-subjects factor and group (in-phase group, anti-phase group, sham stimulation group) as a between-subjects factor was performed to evaluate the effect of dual-site tACS on the ERD values in ST and CT, respectively. In addition, we calculated ERD values of the pre-tACS block for all thirty-six subjects and used paired t-test to compare the ERD values between ST and CT in mu and beta frequency bands.

Furthermore, averaged ERD values of μ frequency band for each electrode were interpolated separately into a topographic map to obtain the spatial distribution of cortex activation in the ST and CT. The cluster-based permutation approach was used to identify topographical patterns with significant interaction effects between block and group in each MI-related task. The threshold used to determine significant electrode clusters was set to 0.05 (p $<$ 0.05).

H. Functional Connectivity Analysis

In order to understand the impact of the stimulation conditions on functional connectivity pattern, we computed the weighted pairwise phase consistency (wPPC) between each pair of EEG recording electrodes. wPPC is a method to estimate the phase consistency across trials and is less sensitive to trial count, making it unbiased even the trial pool is small [42]. In this study, the wPPC was calculated using the function ft_connectivity_ppc.m implemented in Fieldtrip toolbox [43]. The formula of wPPC is as follows:

$$wPPC = \frac{\left|\sum_{k=1}^{n} S_{xy}(f,t)\right|^2 - \sum_{k=1}^{n}\left|S_{xy}(f,t)\right|^2}{\left|\sum_{k=1}^{n}\left|S_{xy}(f,t)\right|\right|^2 - \sum_{k=1}^{n}\left|S_{xy}(f,t)\right|^2} \quad (2)$$

where $S_{xy}(f,t)$ indicates the cross-spectral density of EEG signal between electrodes x and y at frequency f and time t. The greater the wPPC value, the greater the phase consistency between electrodes. Functional connectivity analysis based on wPPC were performed in ST and CT, respectively. For each stimulation condition, wPPC values of each block were calculated from EEG data within task period of [2] and [6] s and frequency range of mu (8-12 Hz) in MI task trials. In order to quantify changes in functional connectivity between the frontoparietal regions, we averaged wPPC values between right frontal and parietal electrodes (F2-P2, F2-P4, F2-P6, F4-P2, F4-P4, F4-P6, F6-P2, F6-P4, F6-P6) in pre-tACS and post-tACS blocks, respectively. Following that, a mixed design
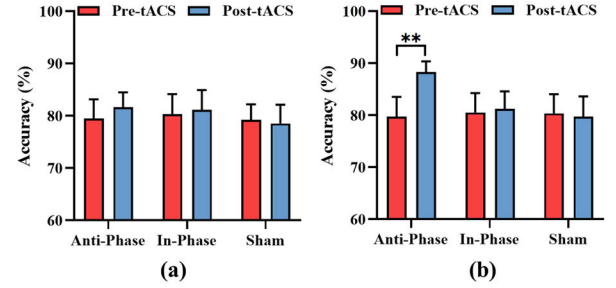

Fig. 3. Classification accuracy between MI-related state and rest state. (a) Accuracy results of ST. (b) Accuracy results of CT. Error bars represent standard error of mean. '**' indicates p $<$ 0.01.

ANOVA was conducted on the resulting mean wPPC values. Furthermore, we calculated normalized wPPC (wPPCz) values to characterize the event-related FC between each pair of electrodes. The wPPCz values were computed by subtracting the wPPC value of baseline period $[-1, 0]$ s from the task period wPPC value and divided it by the standard deviation of baseline period wPPC value. In this case, EEG data from 30 recording electrodes were selected to construct an event-related FC network. These 30 electrodes are overlying the frontal, sensorimotor and parietal areas and include F line electrodes (F1~F6), FC line electrodes (FC1~FC6), C line electrodes (C1~C6), CP line electrodes (CP1~CP6) and P line electrodes (P1~P6). For each pair of electrodes, we calculated the difference in wPPCz values between pre-tACS and post-tACS blocks. After that, a permutation test based on the t-statistic (5000 permutations) was then used to determine the statistical significance of non-zero wPPCz difference. The statistical threshold p-value was set at 0.005 to control multiple comparisons [44]. Similarly, we measured the mean wPPCz values between the right frontal (F2, F4, F6) and parietal (P2, P4, P6) electrodes in the pre-tACS and post-tACS blocks and performed statistical analysis on the obtained mean wPPCz values. In addition, to compare the event-related FC patterns between ST and CT, we constructed event-related FC networks during the pre-tACS block for all thirty-six subjects in ST and CT, respectively. Likewise, electrode pairs with significant non-zero wPPCz value were identified by the permutation test.

I. Statistical Analysis

A mixed design 2×3 ANOVA with block (pre-tACS block, post-tACS block) as a within-subjects factor and group (in-phase group, anti-phase group, sham stimulation group) as a between-subjects factor was applied to analyze the classification accuracy, ERD values, wPPC values and wPPCz values in ST and CT, respectively. Whenever the interaction effect was found to be significant, Bonferonni post-hoc tests was conducted to test for significant differences between blocks in each group. The p-values below the 0.05 was considered as significant.

III. RESULTS

A. Classification Accuracy

In order to evaluate whether stimulation makes EEG patterns during MI more distinguishable, we compared the
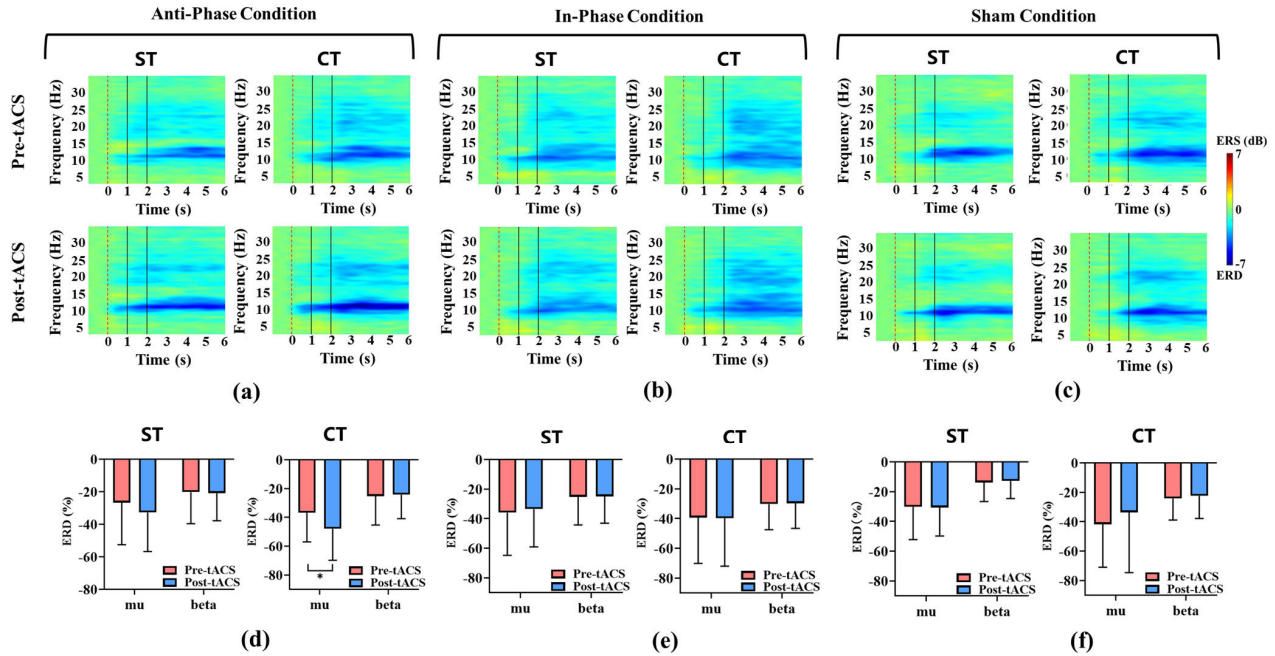
Fig. 4. Time-frequency analysis of contralateral key electrode (C4) in the three conditions. (a) Grand averaged time-frequency maps of ERSP values for the ST and CT in the anti-phase condition. The period [2], [6] s indicates the MI tasks. (b) Grand averaged time-frequency maps in the in-phase condition. (c) Grand averaged time-frequency maps in the sham condition. (d) Grand averaged ERD values of electrode C4 for the ST and CT in the anti-phase condition. The ERD values were averaged in the time segment of [2], [6] s and in the frequency band of mu (8-12 Hz) and beta (14-30 Hz). (e) Grand averaged ERD values in the in-phase condition. (f) Grand averaged ERD values in the sham condition. Error bars represent the standard deviation. '∗' indicates p < 0.05.

classification accuracy among three stimulation groups. The offline accuracies of distinguishing MI-related state from rest state are presented in Fig. 3. For ST vs. Rest classifier, a 2×3 (block $\times$ group) mixed design ANOVA indicated that there was no significant block by group interaction on classification accuracy (F(2,33)=0.477, p=0.625). The main effect of group factor (F(2,33)=0.095, p=0.91) and block factor (F(1,33)=0.396, p=0.533) were also not significant. However, statistical analysis ascertained a significant block $\times$ group interaction on classification accuracy of CT vs. Rest classifier (F(2,33)=4.998, p=0.013). Bonferonni post-hoc comparison revealed that the accuracy in post-tACS block was significantly higher than that in pre-tACS block for the anti-phase group (88.31% $\pm$ 7.04% vs. 79.71% $\pm$ 13.17%, p<0.01). In contrast, no significant difference in accuracy was found between pre-tACS block and post-tACS block in the in-phase (pre-tACS: 80.51% $\pm$ 12.95%, post-tACS: 81.21% $\pm$ 11.71%, p=0.757) and sham (pre-tACS: 80.37% $\pm$ 12.77%, post-tACS: 79.71% $\pm$ 13.5%, p=0.771) stimulation groups. In addition, simple effects analysis confirmed that the CT vs. Rest classifier accuracy in the pre-tACS block was not significant different across three groups (F(2,33)=0.13, p=0.987).

B. Task-Related Desynchronization

In order to understand the effect of stimulation on MI cortical activity, we analyzed the changes in EEG band power before and after three stimulation conditions (in-phase, anti-phase, sham). The grand-averaged time-frequency maps of ERSP values at electrode C4 (in the contralateral hemisphere)

are presented in Fig. 4(a-c). As shown in Fig. 4(a-c), a clear ERD was observed in mu and beta frequency bands during both pre-tACS and post-tACS blocks for all three groups. For anti-phase stimulation group, the ERD in μ band was more pronounced during the post-tACS block compared with the pre-tACS block in both ST and CT. However, the ERD patterns of the in-phase and sham stimulation groups were similar between the pre-tACS and post-tACS blocks, regardless of ST or CT.

Furthermore, we compared the averaged ERD values across the stimulation conditions and blocks to quantify the effectiveness of stimulation on cortical activation (Fig. 4(d-f)). In the mu rhythm, a 2×3 (block $\times$ group) mixed design ANOVA revealed a significant block by group interaction for averaged ERD values in CT (F(2,33)=3.66, p=0.037), but not in ST (F(2,33)=0.851, p=0.436). Bonferonni post-hoc test for CT highlighted that the averaged ERD value was significantly smaller in the post-tACS block compared with the pre-tACS block only in the anti-phase stimulation group (p=0.035). For the in-phase and sham stimulation groups, no significant changes were observed in the averaged ERD values between the pre-tACS and post-tACS blocks (in-phase: p=0.948; sham: p=0.117). In addition, tests of simple effects confirmed that there was no significant difference in CT-related averaged ERD values in the pre-tACS block among three groups (F(2,33)=0.1, p=0.905). For ST, the statistical analysis revealed that there was no significant main effect of group (F(2,33)=0.169, p=0.845) or block (F(1,33)=0.264, p=0.611). For averaged ERD values in the beta rhythm, a 2×3 (block $\times$ group) mixed design ANOVA indicated no
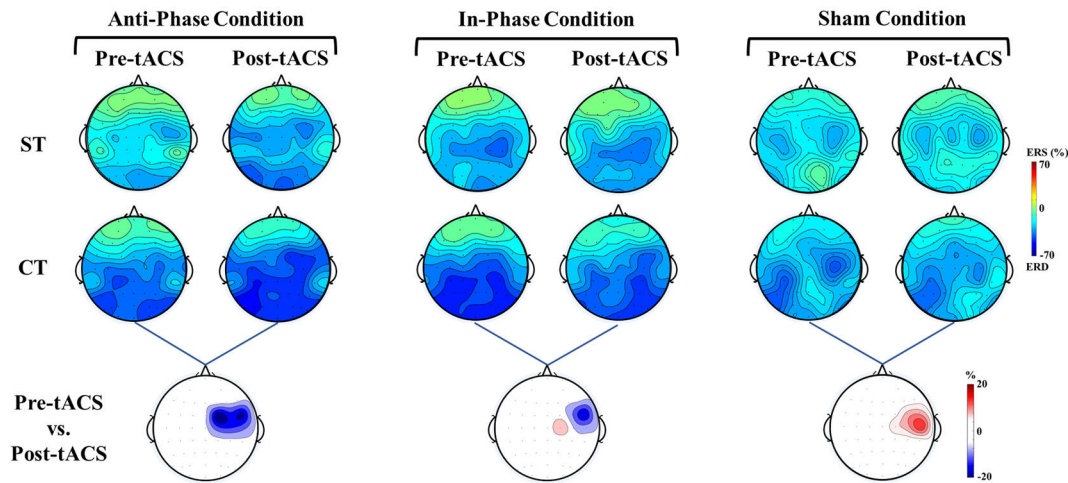
Fig. 5. The grand average ERD topographical maps of pre-tACS and post-tACS blocks for ST and CT in the three stimulation conditions. The first row shows the average spatial distributions of ERD values for ST. The depicted ERD values are averaged in the time segment of [2], [6] s and in the frequency band of mu (8-12 Hz). The second row shows the average spatial distributions of ERD values for CT. The third row shows the significant ERD differences between pre-tACS and post-tACS blocks for CT.

significant interaction between group and block in both ST $(F(2,33)=0.096, p=0.908)$ and CT $(F(2,33)=0.057, p=0.945)$. In addition, there was no significant main effect of group factor (ST: $F(2,33)=1.687$, $p=0.201$; CT: $F(2,33)=0.564$, $p=0.574$) or block factor (ST: $F(1,33)=0.025$, $p=0.877$; CT: $F(1,33)=0.463$, $p=0.501$). For the comparison of ERD values between ST and CT in the pre-tACS block, paired t-test confirmed that ERD values were significantly smaller during CT than during ST in the mu ($p<0.01$) and beta ($p<0.01$) rhythms.

The grand average topographical distribution maps of the pre-tACS and post-tACS blocks for all three groups are presented in Fig. 5. We observed that the ERD patterns over sensorimotor areas were more pronounced during CT than during ST in the mu rhythm, regardless of in-phase, anti-phase or sham stimulation group. For the CT, the ERD patterns of mu rhythm were enhanced in the right sensorimotor area after the anti-phase stimulation, but not after either the in-phase or sham stimulations, suggesting that anti-phase stimulation result in greater activation of contralateral sensorimotor area. Furthermore, the cluster-based permutation test revealed a significant interaction between the block factor and the group factor on the mu rhythm ERD patterns in the right sensorimotor area (FC2, FC4, FC6, C2, C4, C6). In the anti-phase group, the ERD was significantly stronger in the post-tACS block than in the pre-tACS block. However, for the in-phase group, the ERD patterns of the post-tACS block did not show a consistent increase in the right sensorimotor area as compared to the pre-tACS block. For the sham stimulation group, the ERD patterns of the post-tACS block were significantly weaker than that of the pre-tACS block. During ST, a clear ERD pattern appeared in the right sensorimotor area in the mu rhythm of both blocks for all three groups. For the anti-phase group, the activation of the sensorimotor areas was stronger in the post-tACS block compared with the pre-tACS block in the mu rhythm. However, for the in-phase and sham stimulation groups, there
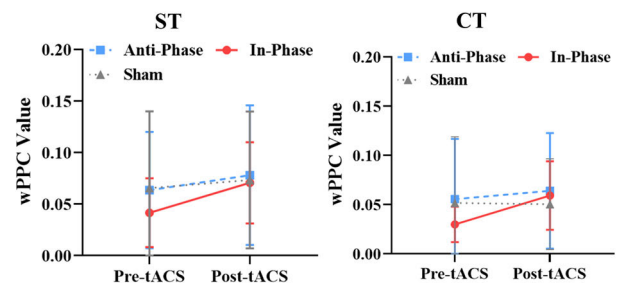

Fig. 6. Mean wPPC values before and after stimulation for the three stimulation conditions. The wPPC values of the electrode pairs between the right frontal (F2, F4, F6) and parietal (P2, P4, P6) regions were averaged. Error bars represent the standard deviation.

was no obvious enhancement in ERD patterns of contralateral sensorimotor region after dual-site tACS. In addition, the cluster-based permutation test indicated that no significant interaction between group and block for topographical patterns in the mu rhythm.

C. Functional Connectivity Results

The mean wPPC values between the frontoparietal regions are presented in Fig. 6. The 2×3 (block $\times$ group) mixed design ANOVA showed no significant block by group interaction for wPPC values in both ST $(F(2,33)=1.553, p=0.227)$ and CT $(F(2,33)=1.656, p=0.206)$. For ST, the main effect of block factor was significant $(F(1,33)=11.802, p<0.01)$, but no main effect of group factor $(F(2,33)=0.25, p=0.78)$. For CT, the statistical analysis revealed that the main effects of both group factor $(F(1,33)=3.044, p=0.09)$ and block factor $(F(2,33)=0.331, p=0.721)$ were not significant.

Fig. 7 shows the event-related functional connectivity alterations between pre-tACS and post-tACS blocks in each group. For the anti-phase group, CT-related connectivity of the bilateral frontoparietal network was significantly decrease during the post-tACS block compared with the pre-
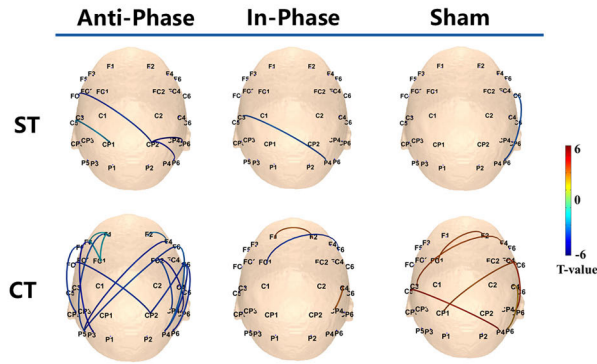
Fig. 7. Statistical contrast maps of event-related functional connectivity between pre-tACS block and post-tACS block in the three conditions. The blue lines in maps represent significantly smaller event-related functional connection in the post-tACS block compared to the pre-tACS block.

tACS block. However, ST-related connectivity between the frontoparietal regions was not significantly reduced in the post-tACS block. For the in-phase group, no significant difference was found in the event-related FC of the frontoparietal network between pre-tACS and post-tACS blocks, regardless of ST or CT. In addition, we found that CT-related connectivity of right frontoparietal network in the post-tACS block was stronger than that in the pre-tACS block for the sham stimulation group. To further test the effect of stimulation on event-related FC, we ran a 2×3 (block $\times$ group) mixed design ANOVA on wPPCz values of contralateral frontoparietal network (Fig. 8). Statistical analysis confirmed that there was a significant block by group interaction in CT ($F_{(2,33)}=5.184$, $p=0.011$). Bonferonni post-hoc test for anti-phase group highlighted that wPPCz value was significantly less in the post-tACS block compared with the pre-tACS block ($p<0.01$). However, no significant different was identified between post-tACS block and pre-tACS block in the in-phase ($p=0.336$) and sham ($p=0.74$) stimulation groups. Additionally, simple effects test did not find significant difference in wPPCz values among three groups in the pre-tACS block ($F_{(2,33)}=1.403$, $p=0.26$). For ST, there was no significant block $\times$ group interaction on wPPCz values ($F_{(2,33)}=0.397$, $p=0.676$), and no main effect of group factor ($F_{(2,33)}=0.172$, $p=0.843$) or block factor ($F_{(1,33)}=0.01$, $p=0.921$). Furthermore, by comparing event-related FC networks between ST and CT, we found that the number of event-related FC in CT was much higher than that in ST (Fig. 9). Notably, the phase consistency of mu rhythm during the MI state was smaller than that during the rest state, regardless of ST or CT.

IV. DISCUSSION

By applying dual-site tACS with a phase difference of 180° (anti-phase) and 0° (in-phase) in the mu range to frontoparietal network, we investigated whether neural response and classification performance during MI can be influenced by modulating inter-regional oscillatory coupling between the frontal and parietal regions. Our results demonstrated that anti-phase tACS stimulation led to an improvement in event-related desynchronization of mu rhythm and classification accuracy during complex MI task. The event-related functional connectivity of the frontoparietal network was also modulated by anti-phase tACS. However, dual-site tACS did not affect sensorimotor cortical activation and classification accuracy in the simple MI task. We provide a direct demonstration of the role of anti-phase synchronization in a high complexity MI task.

A. Anti-Phase tACS in the Frontoparietal Network Has Beneficial Effects on Performance of Complex Task

Motor imagery is defined as a mental rehearsal of a special movement without any overt motor output, which reflects high-level aspects of action planning [23]. Previous studies have revealed that information of MI is associated with activation patterns in the frontoparietal regions [6], [7]. Furthermore, functional connectivity changes across the frontoparietal network also plays an important role in the achievement of MI [24], [25], [26]. Recently, functional relationship between brain regions has been reported to be potentially affected by dual-site tACS. Specifically, it was expected that in-phase stimulation would cause synchronization between target regions, whereas anti-phase stimulation would cause desynchronization [45], [46].

An in-phase tACS has been shown to facilitate inter-regional synchronization by reducing the phase-lag between stimulation sites [32]. Several studies have found that theta in-phase stimulation targeting the frontoparietal network improves performance of working memory tasks [19], [31], [47]. Although not mentioned in these studies, an increasement of working memory performance is typically considered to be accompanied by an increase in theta oscillatory power [48], [49], [50]. Thus, it appears that in-phase stimulation is related with an increase in oscillatory power in the stimulated frequency band. However, it has been shown that MI is associated with decrease in mu band power. As a result, a dual-site tACS with zero-phase lag may not be appropriate for MI tasks. This viewpoint is consistent with our results that there was no significant change in ERD patterns or classification accuracy during MI before and after in-phase tACS. In contrast, we found that the desynchronization of mu rhythms in the CT task was significantly larger after anti-phase tACS. Anti-phase stimulation acting on two distant brain regions simultaneously with waveforms that have 180° phase offset. Unlike in-phase stimulation, tACS studies have shown that anti-phase stimulation does not improve working memory performance and may even deteriorate it [19], [31]. Violante et al. suggested that the variation in the effect between two stimulation conditions may be due to the different functional connectivity patterns modulated by the in-phase and anti-phase stimulations [19]. However, the present results showed no significant effect of stimulation factor on function connectivity between frontal and parietal regions. Therefore, the enhancement of motor-related cortical excitability after anti-phase stimulation observed in the present study may not be simply attributable to functional connectivity changes in the frontoparietal network.

Our results suggest that the increased sensorimotor cortical activation may be associated with a decrease in event-related
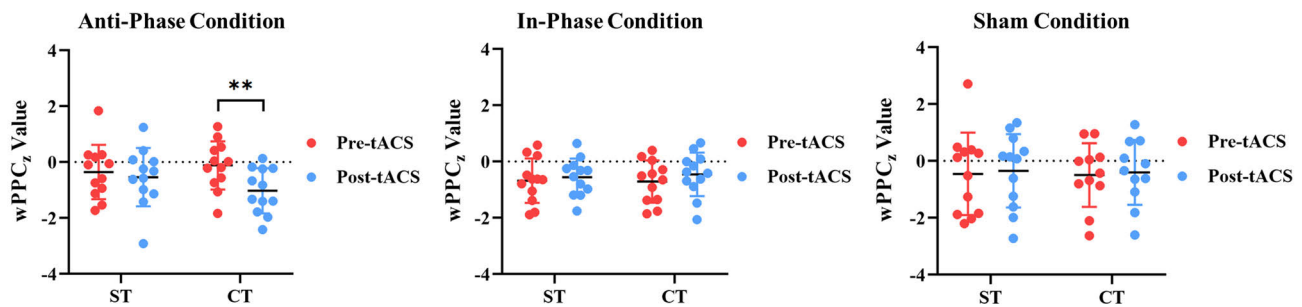
Fig. 8. Mean wPPC$_z$ values before and after stimulation for the anti-phase, in-phase and sham stimulation conditions. Error bars represent the standard deviation. '**' indicates p < 0.01.
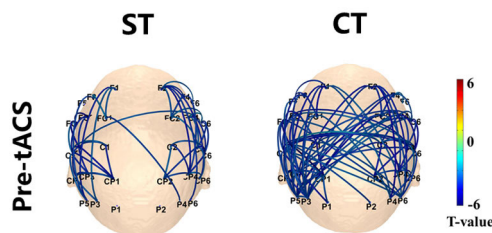

Fig. 9. Event-related functional connectivity network for ST and CT in pre-tACS block. The blue lines in maps represent significantly smaller functional connection during MI compared to resting baseline.

functional connectivity in the frontoparietal network. In the present study, event-related FC was obtained by measuring the FC dissimilarities between MI task and rest. The event-related FC characterizes the brain network reconfiguration from rest to task states and plays an important role in the information processing during MI [51], [52]. Li et al. indicated that functional connectivity linking the frontal and parietal areas decreased during brain reconfiguration associated with the MI [51]. In addition, a higher degree of reconfigured network corresponds to a stronger mu rhythm desynchronization during MI [51]. In our previous study, we also found that the functional connectivity of the frontoparietal network decreased during motor imagery compared to the rest state [53]. A possible underlying mechanism for brain reconfiguration during MI is the reallocation of limited brain resources, in which the strength of task-independent functional connectivity in the frontoparietal network is decreased [51]. Similarly, Mylonas et al. showed that reduced functional connectivity in the alpha band during a sensorimotor task reflected the suppression of processes unrelated to the task [54]. Indeed, BOLD signals associated with alpha phase-locking synchronization during resting state are found in the default mode network [55], which involves a set of widely distributed brain regions in the parietal, temporal and frontal cortex [56]. Therefore, decreased functional connectivity during MI relative to the rest state may be intended to facilitate task completion. This hypothesis is consistent with the results that the event-related FC between frontoparietal regions during CT was significantly smaller after anti-phase stimulation, whereas ERD patterns and classification accuracy were significantly larger in the post-tACS block than in the

pre-tACS block. The positive effect of anti-phase stimulation on MI performance may be attributed to its facilitation of the FC pattern updates from rest to task states. Typically, in-phase stimulation is assumed to increase coordination between the two regions whereas anti-phase stimulation leads to an inter-regional disorganization [32], [45], [46]. The reduced inter-regional coordination caused by anti-phase stimulation may make the network easier to reconfigure. Furter studies are required to confirm this specific hypothesis. In addition, Salamanca-Giron et al. suggested that anti-phase stimulation could generate more dynamical changes in electrical field distribution [18]. Alekseichuk et al. compared the electrical field dynamics in non-human primates receiving 10 Hz in-phase and anti-phase stimulation over prefrontal and occipital areas [57]. The results showed that anti-phase caused a larger electrical field strength and a unidirectional electrical field, whereas in-phase stimulation produced a lower electrical field magnitude and bidirectional electrical fields. These findings may explain the event-related FC changes in CT that we observed only after anti-phase stimulation but not after in-phase stimulation.

B. Anti-Phase Stimulation Has Different Effects on Simple and Complex Tasks

The present positive effects of anti-phase tACS on mu rhythm ERD and MI-BCI classification accuracy were observed only in complex task but not in simple task. This finding reflects that the effectiveness of anti-phase tACS on the MI tasks may be influenced by the cognitive load associated with MI. Indeed, previous studies have reported that the effects of dual-site tACS on task performance are associated with working memory load. Violante et al. indicated that synchronization induced by in-phase stimulation only enhanced behavioral performance when cognitive demands of task was high [19]. Similarly, Draaisma et al. found that theta in-phase tACS applied to the frontoparietal network only improved performance on task with high working memory load, but not with low working memory load [47]. Similar results were also reported by Hu et al. [58]. One possible interpretation of these findings is that the effect of the stimulation highly dependent on the underlying brain state. The effect of tACS is more pronounced when the induced oscillatory changes match the endogenous rhythm activity

engaged in task. Our results showed that the ERD patterns of mu rhythm during complex task were significantly larger than those during simple task. The more obvious ERD patterns in complex task may involve more efficient brain reconfiguration [56], which is more easily affected by anti-phase stimulation. On the other hand, Glover and Baran's motor-cognitive model proposes that motor imagery contains both motor and cognitive properties [59]. Compared with grasping task, writing task require more elaborate motor planning and precise motor control, which may make writing imagery more involved in cognitive than motor networks. Since the frontoparietal network is associated with brain cognitive activities, the modulatory effect of anti-phase tACS may be more likely to affect writing task that is closely related to the cognitive network.

C. Limitations

The present study aimed to investigate the effect of dual-site tACS over the frontoparietal regions on MI-BCI performance. Some limitations of this study need to be mentioned. First, the montage chosen for placing the stimulation electrodes in this study may result in a relatively large area of stimulation. As stated by Saturnino et al., the montage used in present study has more non-focal stimulation compared with the two centre-surround ring montage [45]. Therefore, it is worthwhile in further research to try to use different electrode montages to explore to what extent electrode montages affect task performance. Second, although we chose a fixed frequency stimulation in this study, the optimal stimulation frequency may vary from individual to individual. Comparing fixed-frequency and personalized-frequency stimulation in further studies may enable us to better understand the underlying mechanisms of dual-site tACS. Third, we selected writing imagery as a complex task and grasping imagery as a simple task according to Mashat et al.' study [37]. Although, anti-phase tACS had a positive effect on the writing task in present study, we are currently unable to conclude whether the effect of anti-phase stimulation exists in other MI tasks with high cognitive load. The influence of anti-phase stimulation on various MI tasks needs to be investigated in the future. In addition, this study focused on the effect of dual-site tACS on MI tasks, and it would be interesting to explore the influence of dual-site tACS on behavioral metrics of motor execution in future studies.

V. CONCLUSION

The present study investigated the after-effects of dual-site tACS applied to the frontoparietal regions on the simple and complex MI tasks. Our findings demonstrated that both the ERD patterns and the BCI performance in the complex task were improved after anti-phase stimulation. Meanwhile, anti-phase stimulation resulted in reduced event-related functional connectivity of the frontoparietal network in complex MI task, and this reduction may be associated with more efficient brain reconfiguration. However, we found no significant after-effect of dual-site tACS on ERD patterns and BCI accuracy in the simple MI task. These results altogether indicated that dual-site tACS based anti-phase lag may be promising to improve

sensorimotor cortical activation and MI-BCI performance in the demanding MI task.

REFERENCES

[1] M. Jeannerod, "The representing brain: Neural correlates of motor intention and imagery," *Behav. Brain Sci.*, vol. 17, no. 2, pp. 187–202, Jun. 1994.

[2] J. Munzert, B. Lorey, and K. Zentgraf, "Cognitive motor processes: The role of motor imagery in the study of motor representations," *Brain Res. Rev.*, vol. 60, no. 2, pp. 306–326, May 2009.

[3] T. E. MacIntyre, C. R. Madan, A. P. Moran, C. Collet, and A. Guillot, "Motor imagery, performance and motor rehabilitation," *Prog Brain Res.*, vol. 240, pp. 141–159, Oct. 2018.

[4] J. Wolpaw, N. Birbaumer, D. McFarland, G. Pfurtscheller, and T. Vaughan, "Brain–computer interfaces for communication and control," *Clin. Neurophys.*, vol. 113, no. 6, pp. 767–791, 2002.

[5] R. Foong et al., "Assessment of the efficacy of EEG-based MI-BCI with visual feedback and EEG correlates of mental fatigue for upper-limb stroke rehabilitation," *IEEE Trans. Biomed. Eng.*, vol. 67, no. 3, pp. 786–795, Mar. 2020.

[6] S. Pilgramm et al., "Motor imagery of hand actions: Decoding the content of motor imagery from brain activity in frontal and parietal motor areas," *Hum. Brain Mapping*, vol. 37, no. 1, pp. 81–93, Jan. 2016.

[7] F. Malouin, C. L. Richards, P. L. Jackson, F. Dumas, and J. Doyon, "Brain activations during motor imagery of locomotor-related tasks: A PET study," *Hum. Brain Mapping*, vol. 19, no. 1, pp. 47–62, May 2003.

[8] B. Z. Allison and C. Neuper, "Could anyone use a BCI?" in *Brain-Computer Interfaces*. London, U.K.: Springer, 2010, pp. 35–54.

[9] T. Qu, J. Jin, R. Xu, X. Wang, and A. Cichocki, "Riemannian distance based channel selection and feature extraction combining discriminative time-frequency bands and Riemannian tangent space for MI-BCIs," *J. Neural Eng.*, vol. 19, no. 5, Sep. 2022, Art. no. 056025.

[10] X. Zhao, H. Zhang, G. Zhu, F. You, S. Kuang, and L. Sun, "A multi-branch 3D convolutional neural network for EEG-based motor imagery classification," *IEEE Trans. Neural Syst. Rehabil. Eng.*, vol. 27, no. 10, pp. 2164–2177, Oct. 2019.

[11] T. Corbet, I. Iturrate, M. Pereira, S. Perdikis, and J. D. R. Millán, "Sensory threshold neuromuscular electrical stimulation fosters motor imagery performance," *NeuroImage*, vol. 176, pp. 268–276, Aug. 2018.

[12] X. Shu et al., "Tactile stimulation improves sensorimotor rhythm-based BCI performance in stroke patients," *IEEE Trans. Biomed. Eng.*, vol. 66, no. 7, pp. 1987–1995, Jul. 2019.

[13] M. A. Nitsche and W. Paulus, "Sustained excitability elevations induced by transcranial DC motor cortex stimulation in humans," *Neurology*, vol. 57, no. 10, pp. 1899–1901, Nov. 2001.

[14] B. S. Baxter, B. J. Edelman, N. Nesbitt, and B. He, "Sensorimotor rhythm BCI with simultaneous high definition-transcranial direct current stimulation alters task performance," *Brain Stimulation*, vol. 9, no. 6, pp. 834–841, Nov. 2016.

[15] J. Xie et al., "Enhancement of event-related desynchronization in motor imagery based on transcranial electrical stimulation," *Frontiers Hum. Neurosci.*, vol. 15, Mar. 2021, Art. no. 635351.

[16] C. Wach, V. Krause, V. Moliadze, W. Paulus, A. Schnitzler, and B. Pollok, "Effects of 10 Hz and 20 Hz transcranial alternating current stimulation (tACS) on motor functions and motor cortical excitability," *Behav Brain Res.*, vol. 241, pp. 1–6, Mar. 2013.

[17] M. Feurra, P. Pasqualetti, G. Bianco, E. Santarnecchi, A. Rossi, and S. Rossi, "State-dependent effects of transcranial oscillatory currents on the motor system: What you think matters," *J. Neurosci.*, vol. 33, no. 44, pp. 17483–17489, Oct. 2013.

[18] R. F. Salamanca-Giron et al., "Enhancing visual motion discrimination by desynchronizing bifocal oscillatory activity," *NeuroImage*, vol. 240, Oct. 2021, Art. no. 118299.

[19] I. R. Violante et al., "Externally induced frontoparietal synchronization modulates network dynamics and enhances working memory performance," *Elife*, vol. 6, Mar. 2017, Art. no. e22001.

[20] A. Pooresmaeili, J. Poort, and P. R. Roelfsema, "Simultaneous selection by object-based attention in visual and frontal cortex," *Proc. Nat. Acad. Sci. USA*, vol. 111, no. 17, pp. 6467–6472, Apr. 2014.

[21] C. A. Bosman et al., "Attentional stimulus selection through selective synchronization between monkey visual areas," *Neuron*, vol. 75, no. 5, pp. 875–888, Sep. 2012.

[22] T. P. Zanto and A. Gazzaley, "Fronto-parietal network: Flexible hub of cognitive control," *Trends Cognit. Sci.*, vol. 17, no. 12, pp. 602–603, Dec. 2013.

[23] T. Zhang et al., "Structural and functional correlates of motor imagery BCI performance: Insights from the patterns of fronto-parietal attention network," *NeuroImage*, vol. 134, pp. 475–485, Jul. 2016.

[24] T. Ogawa, H. Shimobayashi, J.-I. Hirayama, and M. Kawanabe, "Asymmetric directed functional connectivity within the frontoparietal motor network during motor imagery and execution," *NeuroImage*, vol. 247, Feb. 2022, Art. no. 118794.

[25] S. Bajaj, A. J. Butler, D. Drake, and M. Dhamala, "Brain effective connectivity during motor-imagery and execution following stroke and rehabilitation," *NeuroImage, Clin.*, vol. 8, pp. 572–582, Jun. 2015.

[26] Q. Gao, X. Duan, and H. Chen, "Evaluation of effective connectivity of motor areas during motor imagery and execution using conditional Granger causality," *NeuroImage*, vol. 54, no. 2, pp. 1280–1288, Jan. 2011.

[27] P. Sauseng and W. Klimesch, "What does phase information of oscillatory brain activity tell us about cognitive processes?" *Neurosci. Biobehavioral Rev.*, vol. 32, no. 5, pp. 1001–1013, Jul. 2008.

[28] F. Varela, J.-P. Lachaux, E. Rodriguez, and J. Martinerie, "The brainweb: Phase synchronization and large-scale integration," *Nature Rev. Neurosci.*, vol. 2, no. 4, pp. 229–239, Apr. 2001.

[29] J. Daume, T. Gruber, A. K. Engel, and U. Friese, "Phase-amplitude coupling and long-range phase synchronization reveal frontotemporal interactions during visual working memory," *J. Neurosci.*, vol. 37, no. 2, pp. 313–322, Jan. 2017.

[30] A. Von Stein and J. Sarnthein, "Different frequencies for different scales of cortical integration: From local gamma to long range alpha/theta synchronization," *Int. J. Psychophysiol.*, vol. 38, no. 3, pp. 301–313, Dec. 2000.

[31] R. Polanía, M. A. Nitsche, C. Korman, G. Batsikadze, and W. Paulus, "The importance of timing in segregated theta phase-coupling for cognitive performance," *Current Biol.*, vol. 22, no. 14, pp. 1314–1318, Jul. 2012.

[32] Z. Yaple and R. Vakhrushev, "Modulation of the frontal-parietal network by low intensity anti-phase 20 Hz transcranial electrical stimulation boosts performance in the attentional blink task," *Int. J. Psychophysiol.*, vol. 127, pp. 11–16, May 2018.

[33] R. Polanía, M. Moisa, A. Opitz, M. Grueschow, and C. C. Ruff, "The precision of value-based choices depends causally on fronto-parietal phase coupling," *Nature Commun.*, vol. 6, no. 1, pp. 1–10, Aug. 2015.

[34] T. Neuling, S. Rach, and C. S. Herrmann, "Orchestrating neuronal networks: Sustained after-effects of transcranial alternating current stimulation depend upon brain states," *Frontiers Hum. Neurosci.*, vol. 7, p. 161, Apr. 2013.

[35] A. A. S. Alahmadi et al., "Complex motor task associated with non-linear BOLD responses in cerebro-cortical areas and cerebellum," *Brain Struct. Function*, vol. 221, no. 5, pp. 2443–2458, Jun. 2016.

[36] G. B. Saturnino, O. Puonti, J. D. Nielsen, D. Antonenko, K. H. Madsen, and A. Thielscher, "SimNIBS 2.1: A comprehensive pipeline for individualized electric field modelling for transcranial brain stimulation," in *Brain and Human Body Modeling: Computational Human Modeling at EMBC*. Cham, Switzerland: Springer, 2019, pp. 3–25.

[37] M. E. M. Mashat, C. Lin, and D. Zhang, "Effects of task complexity on motor imagery-based brain–computer interface," *IEEE Trans. Neural Syst. Rehabil. Eng.*, vol. 27, no. 10, pp. 2178–2185, Oct. 2019.

[38] A. Delorme and S. Makeig, "EEGLAB: An open source toolbox for analysis of single-trial EEG dynamics including independent component analysis," *J. Neurosci. Methods*, vol. 134, no. 1, pp. 9–21, Mar. 2004.

[39] F. Perrin, J. Pernier, O. Bertnard, M. H. Giard, and J. F. Echallier, "Mapping of scalp potentials by surface spline interpolation," *Electroencephalogr. Clin. Neurophysiol.*, vol. 66, no. 1, pp. 75–81, Jan. 1987.

[40] J. Kayser and C. E. Tenke, "Principal components analysis of Laplacian waveforms as a generic method for identifying ERP generator patterns: II. Adequacy of low-density estimates," *Clin. Neurophysiol.*, vol. 117, no. 2, pp. 369–380, Feb. 2006.

[41] S. Makeig, "Auditory event-related dynamics of the EEG spectrum and effects of exposure to tones," *Electroencephalogr. Clin. Neurophysiol.*, vol. 86, no. 4, pp. 283–293, Apr. 1993.

[42] A. Wilsch, M. J. Henry, B. Herrmann, C. S. Herrmann, and J. Obleser, "Temporal expectation modulates the cortical dynamics of short-term memory," *J. Neurosci.*, vol. 38, no. 34, pp. 7428–7439, Aug. 2018.

[43] R. Oostenveld, P. Fries, E. Maris, and J.-M. Schoffelen, "FieldTrip: Open source software for advanced analysis of MEG, EEG, and invasive electrophysiological data," *Comput. Intell. Neurosci.*, vol. 2011, pp. 1–9, Jan. 2011.

[44] J. K. Kleen et al., "Oscillation phase locking and late ERP components of intracranial hippocampal recordings correlate to patient performance in a working memory task," *Frontiers Hum. Neurosci.*, vol. 10, p. 287, Jun. 2016.

[45] G. B. Saturnino, K. H. Madsen, H. R. Siebner, and A. Thielscher, "How to target inter-regional phase synchronization with dual-site transcranial alternating current stimulation," *NeuroImage*, vol. 163, pp. 68–80, Dec. 2017.

[46] S. Alagapan, J. Riddle, W. A. Huang, E. Hadar, H. W. Shin, and F. Fröhlich, "Network-targeted, multi-site direct cortical stimulation enhances working memory by modulating phase lag of low-frequency oscillations," *Cell Rep.*, vol. 29, no. 9, pp. 2590–2598.e4, Nov. 2019.

[47] L. R. Draaisma, M. J. Wessel, M. Moyne, T. Morishita, and F. C. Hummel, "Targeting the frontoparietal network using bifocal transcranial alternating current stimulation during a motor sequence learning task in healthy older adults," *Brain Stimulation*, vol. 15, no. 4, pp. 968–979, Jul. 2022.

[48] J. Riddle, J. M. Scimeca, D. Cellier, S. Dhanani, and M. D'Esposito, "Causal evidence for a role of theta and alpha oscillations in the control of working memory," *Current Biol.*, vol. 30, no. 9, pp. 1748–1754, May 2020.

[49] T. Popov, P. Popova, M. Harkotte, B. Awiszus, B. Rockstroh, and G. A. Miller, "Cross-frequency interactions between frontal theta and posterior alpha control mechanisms foster working memory," *NeuroImage*, vol. 181, pp. 728–733, Nov. 2018.

[50] O. Jensen and C. D. Tesche, "Frontal theta activity in humans increases with memory load in a working memory task," *Eur. J. Neurosci.*, vol. 15, no. 8, pp. 1395–1399, May 2002.

[51] F. Li et al., "Brain network reconfiguration during motor imagery revealed by a large-scale network analysis of scalp EEG," *Brain Topography*, vol. 32, no. 2, pp. 304–314, Mar. 2019.

[52] D. H. Schultz and M. W. Cole, "Higher intelligence is associated with less task-related brain network reconfiguration," *J. Neurosci.*, vol. 36, no. 33, pp. 8551–8561, Aug. 2016.

[53] L. Zhang, L. Chen, Z. Wang, X. Zhang, X. Liu, and D. Ming, "Enhancing visual-guided motor imagery performance via sensory threshold somatosensory electrical stimulation training," *IEEE Trans. Biomed. Eng.*, vol. 70, no. 2, pp. 756–765, Feb. 2023.

[54] D. S. Mylonas, C. I. Siettos, I. Evdokimidis, A. C. Papanicolaou, and N. Smyrnis, "Modular patterns of phase desynchronization networks during a simple visuomotor task," *Brain Topography*, vol. 29, no. 1, pp. 118–129, Jan. 2016.

[55] K. Jann, T. Dierks, C. Boesch, M. Kottlow, W. Strik, and T. Koenig, "BOLD correlates of EEG alpha phase-locking and the fMRI default mode network," *NeuroImage*, vol. 45, no. 3, pp. 903–916, Apr. 2009.

[56] J. Smallwood, B. C. Bernhardt, R. Leech, D. Bzdok, E. Jefferies, and D. S. Margulies, "The default mode network in cognition: A topographical perspective," *Nature Rev. Neurosci.*, vol. 22, no. 8, pp. 503–513, Aug. 2021.

[57] I. Alekseichuk et al., "Electric field dynamics in the brain during multi-electrode transcranial electric stimulation," *Nature Commun.*, vol. 10, no. 1, pp. 1–10, Jun. 2019.

[58] Z. Hu, I. B. H. Samuel, S. Meyyappan, K. Bo, C. Rana, and M. Ding, "Aftereffects of frontoparietal theta tACS on verbal working memory: Behavioral and neurophysiological analysis," *IBRO Neurosci. Rep.*, vol. 13, pp. 469–477, Dec. 2022.

[59] S. Glover and M. Baran, "The motor-cognitive model of motor imagery: Evidence from timing errors in simulated reaching and grasping.," *J. Exp. Psychol., Hum. Perception Perform.*, vol. 43, no. 7, pp. 1359–1375, 2017.